doi.org/10.36721/PJPS.2026.39.9.258.1

Pharmacokinetic interaction between evodiamine and doxofylline in rats

Yuxian Lin[1,2]*, Yongle Yang[3], Wang Luo[1], Yangfang Chen[1], Feng Chen[1], Zhenyang Zang[1] and Qiulian Tang[1]

[1]The Third Clinical Institute Affiliated to Wenzhou Medical University, Wenzhou People's Hospital, Wenzhou, Zhejiang, China
[2]School of Pharmacy, Key Laboratory of Molecular Pharmacology and Drug Evaluation (Yantai University), Ministry of Education, Collaborative Innovation Center of Advanced Drug Delivery System and Biotech Drugs in Universities of Shandong, Yantai University, Yantai, Shandong, China
[3]Department of Pharmacy, Wenzhou Medical University, Wenzhou, Zhejiang, China

Abstract: **Background**: Doxofylline (DFL) is a medication widely employed in the management of asthma and chronic obstructive pulmonary disease. Evodiamine (EVO), a bioactive alkaloid from traditional Chinese medicine (TCM), is commonly utilized for treating hypertension, gastropathy, and eczema. Cytochrome P450 enzymes primarily mediate the metabolism of both pharmaceuticals and TCMs *in-vivo*, which potentially lead to drug-drug interactions. **Objectives**: This study aimed to investigate the effects of oral EVO on the pharmacokinetics (PK) of DFL and its metabolite, theophylline (TPL), in rats. **Methods**: Twelve rats were randomly assigned to control and experimental groups. The experimental group received 50 mg/kg EVO orally once daily for one week, while the control group received 0.5% sodium carboxymethyl cellulose. On day 7, DFL (80 mg/kg) was administered 2 h post-treatment. Venous blood specimens were collected from the retro-orbital venous plexus at 0.1667, 0.5, 1, 1.5, 2, 3, 4, 6, 8, 12, 24, and 48 h post-dose. Plasma concentrations of DFL and TPL were analyzed by liquid chromatography-tandem mass spectrometry (LC-MS/MS). **Results**: Compared with the control group, the experimental group showed significant alterations in several PK parameters for both DFL and TPL. The administration of EVO markedly increased $MRT_{(0-\infty)}$, $MRT_{(0-t)}$, $VRT_{(0-\infty)}$, $VRT_{(0-t)}$, $t_{1/2z}$, and Vz/F for DFL while also enhancing CLz/F and Vz/F for TPL. Conversely, EVO notably decreased $AUC_{(0-\infty)}$, $AUC_{(0-t)}$, and $MRT_{(0-t)}$ values associated with TPL. **Conclusion**: Concomitant administration of EVO alongside DFL resulted in substantial modifications to key PK parameters concerning both DFL and its metabolite TPL in rats. Specifically, EVO prolonged the retention time and increased the volume of distribution of DFL, while simultaneously reducing the bioavailability and accelerating the clearance of TPL ($P<0.05$). Therefore, it is imperative to closely monitor the impact of TCM EVO on the PKs of DFL and TPL in experimental animals, necessitating further research and clinical observation.

Keywords: Doxofylline; Evodiamine; HPLC-MS/MS; Pharmacokinetics; Theophylline

Submitted on 18-12-2025 – Revised on 14-02-2026 – Accepted on 23-02-2026

INTRODUCTION

Asthma is a complex and heterogeneous respiratory syndrome characterized by persistent airway hyperresponsiveness, obstruction, remodeling, and inflammation. This condition has been a persistent health challenge for millennia and remains a critical global health issue, affecting more than 330 million people and impairing educational attainment and workforce participation worldwide (Papadopoulos *et al.,* 2022). In the United States, asthma prevalence reaches approximately 8% among adults, representing a substantial socioeconomic (Wu *et al*., 2019). Although existing pharmacotherapies can alleviate symptoms, asthma management continues to present considerable challenges, highlighting an urgent need for novel interventions capable of modifying disease progression and preserving long-term lung function.

Evodiamine (EVO) is a natural quinolone alkaloid derived from the fruit of Evodia rutaecarpa (a plant belonging to the Rutaceae family) and is used as a traditional Chinese medicine (TCM). Historically, EVO has been used to treat a wide range of conditions, including vomiting, diarrhea, headaches, abdominal pain, amenorrhea, postpartum hemorrhage, dysmenorrhea, and other related morbidities. The research findings have revealed that EVO exhibits potent pharmacological activities through multiple mechanisms, such as anti-atherosclerotic (Zha *et al.*, 2023), anticancer (Panda *et al*., 2023), antiproliferative (Haiss *et al.*, 2025), anti-inflammatory, immunomodulatory, and antibacterial effects (Wang *et al.*, 2021). Notably, recent research suggests that EVO may protect against asthma by reducing bronchial inflammation and pulmonary structural remodeling, potentially by inhibiting the HMGB1/NF-κB/TLR-4 pathway (Wang *et al.*, 2021). Furthermore, EVO has been shown to suppress the activity of key drug-metabolizing enzymes, including CYP1A2, CYP2C9, and CYP2D6 (Zhang *et al.*, 2016).

DFL, a newer generation xanthine derivative, is recognized for its bronchodilating and anti-inflammatory properties

**Corresponding author:* e-mail: linyuxian0815@126.com

and is prescribed globally for the clinical intervention for asthma and chronic obstructive pulmonary disease (COPD). DFL is distinguished by a higher safety margin compared to theophylline (TPL) and has been shown to be more effective in asthmatic patients, with enhanced bronchodilatory and anti-inflammatory effects (Fierro *et al.*, 2022; Liu *et al*., 2021). Upon oral administration, DFL undergoes rapid absorption, hepatic metabolism, and partial urinary excretion (Rao *et al.*, 2013).

TPL, a metabolite of DFL, is predominantly metabolized *in-vivo* by the cytochrome P450 enzymes (CYP) 1A2 and CYP2E1 (Yang *et al*., 2024). TPL has a narrow therapeutic index, making it susceptible to various side effects and drug-drug interactions, which necessitates monitoring of plasma drug levels to prevent toxicity (Al-Shami *et al., 2025*). Both DFL and TPL are primarily metabolized through CYP1A2 and CYP2E1. Previous research has indicated that the PK parameters of these two substances can be influenced by the concurrent administration of alcohol, presumably by modifying their metabolism via CYP2E1 and alcohol dehydrogenase (ADH) (Yuxian *et al.,* 2015). The blood plasma concentration of TPL in the liver can be affected by allopurinol, oxipurinol, and andrographolide, which interact with CYP1A2 and CYP3A4 (Ma *et al.*, 2016; Li *et al.*, 2013; Yang *et al.*, 2008). Therefore, any compound that impacts these enzymes is likely to alter the metabolism of both DFL and TPL.

In clinical practice, combining DFL with herbal medicine is anticipated to enhance anti-inflammatory effects and improve airway function in asthma patients, potentially overcoming drug resistance, as supported by *in-vivo* studies. Given that both DFL and TPL are metabolized by the same cytochrome P450 enzymes, particularly CYP1A2 (Sun *et al*., 2020; Zhao *et al*., 2020), it is hypothesized that pretreatment with EVO could impact the activity of the CYP family, resulting in herb-drug interactions that could influence the PK of DFL and its metabolite TPL. To date, no studies have yet explored the PK interactions between EVO and DFL. Therefore, it is crucial to investigate the influence of EVO on the PK of DFL and TPL to provide valuable evidence for clinical decision-making.

MATERIALS AND METHODS

Chemicals and instruments

DFL, with a purity of 99.6%, was sourced from Santa Cruz Biotechnology in Canada. TPL, boasting a purity of 99.9%, was acquired from the China Food and Drug Testing and Research Institute. EVO and carbamazepine, both with a purity of 98%, were procured from J&K Scientific Ltd. HPLC-grade acetonitrile was procured from Merck Darmstadt in Germany. Distilled water was generated using a Millipore Milli-Q Plus water purification system. All other reagents were of analytical grade and were sourced from reputable suppliers. The chemical structures of DFL and EVO are shown in Fig. 1.

LC-MS system: Agilent 1290 Infinity Series High Performance Liquid Chromatography System comprising a G1316C Column Oven, G4226 Autosampler, G1330B Column Oven, and G4220A Binary Pump, coupled with an Agilent 6460 Triple Quadrupole Mass Spectrometer.

LC-MS/MS conditions

DFL and TPL were quantified by an Agilent 1,290 series HPLC system coupled to a 6460 triple quadrupole mass spectrometer featuring an electrospray ionization (ESI) source. Plasma samples were processed using liquid-liquid extraction. The chromatographic isolation of the analytes was achieved using a Phenomenex Synergi Polar-RP column (50 mm × 2.0 mm, 4 µm) maintained at 35 ℃. The mobile phase was composed of methanol and water containing 0.1% formic acid (72:38, v/v) and was delivered at a flow rate of 0.2 mL•min^{-1}. The mass spectrometer was operated in positive ionization mode. Selective reaction monitoring (SRM) was employed for the quantification of DFL, TPL, and carbamazepine (internal standard, IS). The SRM transitions were configured as follows: m/z 267.0→181.1 for DFL, 239.0→164.0 for TPL, and 237.2→194.2 for IS (Fang *et al*., 2019). After optimization, the source parameters were fine-tuned to the following settings: a curved desolvation line temperature at 250^{o}C, a heat block temperature at 200^{o}C, and a source voltage of 1.7 kV. The analytical run time was 7.0 min, with an injection volume of 10 µL. The monitoring time for each SRM transition was set to 1.0 s. Data capture and analysis were conducted using the MassHunter workstation. The fragment ion spectra of DFL, TPL, and IS were depicted in Figs. 2A-C.

Calibration and quality control (QC) sample preparation

Methanol was used to prepare 1.0 mg•mL^{-1} stock solutions of DFL, TPL, and IS, which were subsequently stored at 4^{o}C for stability. A set of calibration solutions with varying concentrations for DFL, TPL, and IS was prepared by diluting the reference solutions using the liquid phase. Calibration standards and QC samples were generated using blank rat plasma. The calibration working standards were prepared at final concentrations of 2, 20, 50, 100, 500, 1000, 2000, 3000 ng•mL^{-1} for DFL and 0.1, 1, 2.5, 5, 7.5, 10, 15, and 25 ng•mL^{-1} for TPL in rat blank plasma. For DFL, QC samples in plasma were formulated at 20, 500, and 2000 ng•mL^{-1}, while for TPL, the concentrations were set at 2.5, 7.5, and 15 ng•mL^{-1}.

Plasma sample preparation

100 µL of plasma sample was aliquoted into 5-mL Eppendorf tubes. To each tube, 1.5 mL of a 19:1 (v: v) mixture of dichloromethane and isopropanol was added, followed by 10 µL of the IS working solution at a concentration of 2 µg•mL^{-1}. The sample mixture was vortexed for 30 s, then treated with 1 mL of ethyl acetate and vortexed for 3 min. After centrifugation at 8000 × g for 10 min, the supernatant was carefully collected and evaporated to dryness under a gentle nitrogen stream at

37 ℃. The resulting residue was reconstituted in 500 µl of the eluent by vortexing for 30 s. Finally, a 10-µL aliquot of the supernatant was introduced for LC-MS/MS characterization.

Method validation

The matrix effects (ME) were assessed in accordance with established bioanalytical guidelines (Castillo-Ribelles *et al.*, 2025). Relative ME was assessed by comparing the peak area of the target analyte in spiked blank plasma (postextraction addition) from five independent batches of rats with those from neat standard solutions at identical concentrations. The evaluation was performed at three QC levels (n = 5). Its effect was calculated using the formula: ME (%) = (Ai/Ar) × 100, where Ai represents the analyte peak area in post-spiked plasma and Ar represents the analyte peak area in the neat solution. The same procedure was applied to assess the matrix effect for the IS. The extraction rate was determined by comparing the peak area of the analyte in the extracted fractions to that in the non-extracted samples, both at equivalent concentrations.

Specificity

The analytical method specificity was appraised by examining chromatograms from blank plasma samples sourced from six distinct batches of rats. The assessment aimed to confirm that no endogenous interference occurs at the retention times corresponding to both the analyte and IS.

Linearity and lower limit of quantitation (LLOQ)

To ascertain the linearity of the analytical method, an eight-point calibration series was constructed for DFL in the range of 2.0 to 3,000 ng•mL^{-1} and for TPL in the range of 0.1 to 25 ng•mL^{-1}. These calibration standards were extracted and analyzed independently over three consecutive days. The linearity of the calibration functions for both DFL and TPL was assessed using a weighted (1/x2) least-squares linear regression analysis, with area ratios plotted against the corresponding concentrations. The LLOQ was identified as the initial concentration point on the calibration plots that yielded a response within the quantifiable range.

Precision and accuracy

The analytical method's precision and accuracy were assessed through the analysis of QC samples in blank plasma at three distinct concentration levels: 20, 500, and 2000 ng•mL^{-1} for DFL and 2.5, 7.5, and 15 ng•mL^{-1} for TPL. These assessments were performed over three separate days.

Extraction recovery was evaluated to determine the effectiveness of the method in extracting the analytes from biological matrices. This was accomplished by comparing the chromatographic peak area ratios of the extracted QC samples to those of analytical solutions that were reassembled in blank plasma matrices. A similar approach was used to determine the recovery of the IS.

To guarantee the validity of the findings, the stability of DFL and TPL QC samples was evaluated under the following conditions:

- Exposure to ambient temperature (25 ºC) for 6 h.
- Storage in the automatic sampler at 4 ºC for 24 h.
- Three complete cycles of freezing and thawing.
- Lengthy storage at -20 ºC for 30 consecutive days.

Animal experiment

Male Sprague-Dawley rats, with body weights between 200-220 g (n=12), were purchased from the animal research center of Luye Pharma in Yantai, China. The rats were kept in normal cages under controlled conditions: temperature 18-20 °C, humidity 45-55%, and a 12 h light-dark cycle to simulate a natural day-night pattern. To standardize experimental conditions, rats were deprived of food for 12 h prior to the experiment, but had free access to water. The 12 rats were randomly divided into two groups. Group 1 received a sodium carboxymethyl cellulose (CMC) solution (0.5%, 10 ml•kg^{-1}), and Group 2 was administered EVO (50.0 mg•kg^{-1}) for seven consecutive days. After the administration of CMC or EVO, both groups were given DFL (80.0 mg•kg^{-1}). Blood samples (0.5 mL) were drawn from the suborbital veniplex into heparinized tubes before dosing and at multiple time points afterward: 0.1667, 0.5, 1, 1.5, 2, 3, 4, 6, 8, 12, 24, and 48 h for DFL and TPL. Plasma was isolated via centrifugation at 8000 rpm for 10 min and then kept at -20ºC until follow-up testing.

Pharmacokinetic and statistical evaluation

The sample size was set at n=6 per group. This is consistent with standard practice in preclinical PK studies, which commonly employs this group size to robustly estimate key PK parameters and their variability (Moreira *et al.*, 2020; Campbell *et al.*, 2021). The choice of this minimum feasible number directly adheres to the "3R" principles of animal research, specifically fulfilling the "Reduction" tenet by using the fewest animals necessary to achieve scientific objectives (Harstad *et al.*, 2016). The PK parameters of DFL and its metabolite TPL were determined using non-compartmental analysis with Drug and Statistics (DAS) software (version 3.0, Bontz Inc., Beijing, China). For statistical comparisons between the experimental and control groups, a nonparametric rank-sum test or t-test was applied, depending on the distribution characteristics of the data. Statistical significance was indicated by a p value less than 0.05. The data were analyzed using non-compartmental methods with SPSS software (version 19.0, Chicago, IL). The entire dataset was displayed as means ± standard deviation (SD).

RESULTS

Method verification

Selectivity

The LC-MS/MS chromatograms depicting the presence of EVO on DFL under three distinct conditions are illustrated

in Fig. 2: (A) blank plasma, (B) blank plasma spiked with analytes and IS (B) and (C) actual plasma samples from rats after oral DFL administration. The retention times for DFL, TFL, and the IS were 3.02, 4.04, and 1.54 min, respectively. The analytes and IS were effectively resolved without interference from endogenous compounds at their distinct elution times.

(A)

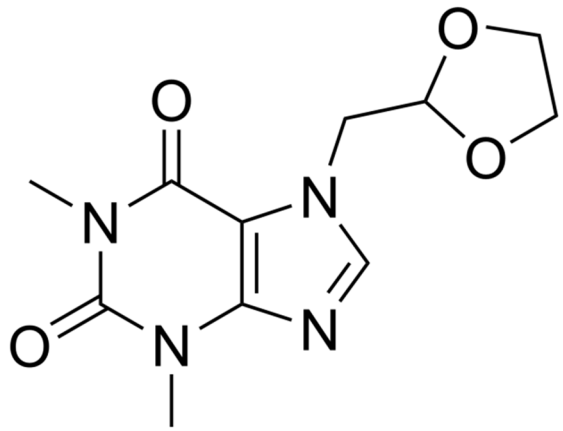

(B)

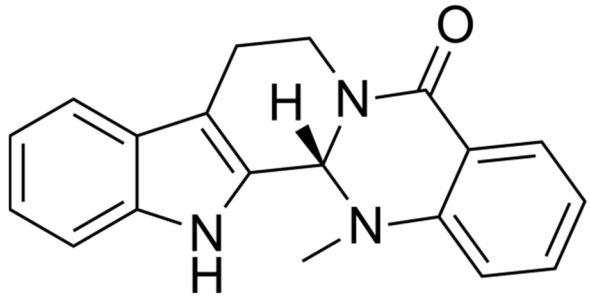

Fig. 1: Chemical structures of (A) doxofylline and (B) evodiamine. (The chemical structure formula of the compounds was downloaded from https://m.chemicalbook.com/ProductIndex.aspx.).

Calibration curve and LLOQ

Linear regression analysis was employed to establish the calibration plots for DFL across the range of 2 to 3,000 ng•mL^{-1} and for TPL over the range of 0.1 to 25 ng•mL^{-1}. The resulting calibration equations were Y = 0.0089X + 0.0977 (r = 0.9986) for DFL and Y = 0.0239X - 0.0104 (r = 0.9963) for TPL. Additionally, the precision (expressed as relative standard deviation, RSD) and accuracy of measured concentrations across all standard curve points, including the LLOQ, were within 15% of the nominal values, matching acceptance criteria.

Precision and accuracy

The precision and accuracy of the analytes are detailed in Table 1, both for intra-day and inter-day measurements. For DFL, intra-day precision ranged from 3.55% to 4.22%, while inter-day precision fluctuated between 2.80% and 6.01%. For TPL, intra-day precision spanned from 2.92% to 4.77%, with inter-day precision ranging from 1.89% to 4.32%. The accuracy for both analytes remained below 10%. The method's precision and accuracy were found to be in compliance with the validation criteria.

Extraction recovery and matrix effect

Table 2 presented that extraction recovery for DFL in plasma samples was above 91.19% and for TPL, it was consistently above 94.08% across all three concentration levels. Furthermore, the relative ME for DFL ranged from 97.00% to 101.08%, while for TPL it varied between 99.30% and 102.11%. In a separate observation, the absolute ME for DFL was between 93.11% and 102.28%, and for TPL, from 98.23% and 105.67%. Consequently, the analytes exhibited satisfactory recoveries and fulfilled the ME requirements.

Stability

The relative error (RE) and RSD values, derived from stability assessments of DFL and TPL in rat plasma, were all within the acceptable limit of ±10% under diverse storage and processing states. These conditions included exposure to ambient temperature for 6 h, storage in the automatic sampler at 4^{o}C for 24 h, three cycles of freezing and thawing, and storage at -20^{o}C for 30 d.

Concentrations of EVO on DFL

Fig. 3 illustrates the mean plasma concentration-time profile of DFL and its metabolite TPL after oral administration, both as a single agent and in combination with multiple doses of EVO. Within the 48 h period post-DFL gavage, the PK curves revealed two distinct absorption peaks for DFL in rats, whereas only a single absorption peak was observed for TPL. Additionally, the DFL concentration was undetectable at the 48 h mark. This suggested that DFL undergoes metabolic conversion more rapidly than TPL *in-vivo*. For specific figures, please refer to Figs. S1 and S2.

Pharmacokinetic parameters of EVO on DFL

The principal PK parameters for DFL and TPL are detailed in Table 3. Upon co-administration of DFL with multiple doses of EVO, significant increases were observed in several parameters compared to the control group: $t_{1/2z}$ by 47.89%, Vz/F by 34.78%, $MRT_{(0-t)}$ by 34.53%, $MRT_{(0-\infty)}$ by 43.19%, $VRT_{(0-t)}$ by 101.76 % and $VRT_{(0-\infty)}$ by 157.49%. In contrast, other PK values for DFL, such as $AUC_{(0-t)}$, $AUC_{(0-\infty)}$, T_{max}, CLz/F, and C_{max}, showed no remarkable differences between the two groups. In addition, the CLz/F of TPL was markedly elevated by 44.56%, while $AUC_{(0-t)}$, $AUC_{(0-\infty)}$, C_{max}, $MRT_{(0-t)}$, and $MRT_{(0-\infty)}$ were significantly decreased by 28.73%, 31.29%, 17.43%, 7.65%, and 11.51%, respectively. However, no statistically significant changes were noted in the $t_{1/2z}$, T_{max}, C_{max}, $VRT_{(0-t)}$, and $VRT_{(0-\infty)}$ of TPL between the groups. For specific data, please refer to Tables S1.1-S1.4 and S2.1-S2.4.

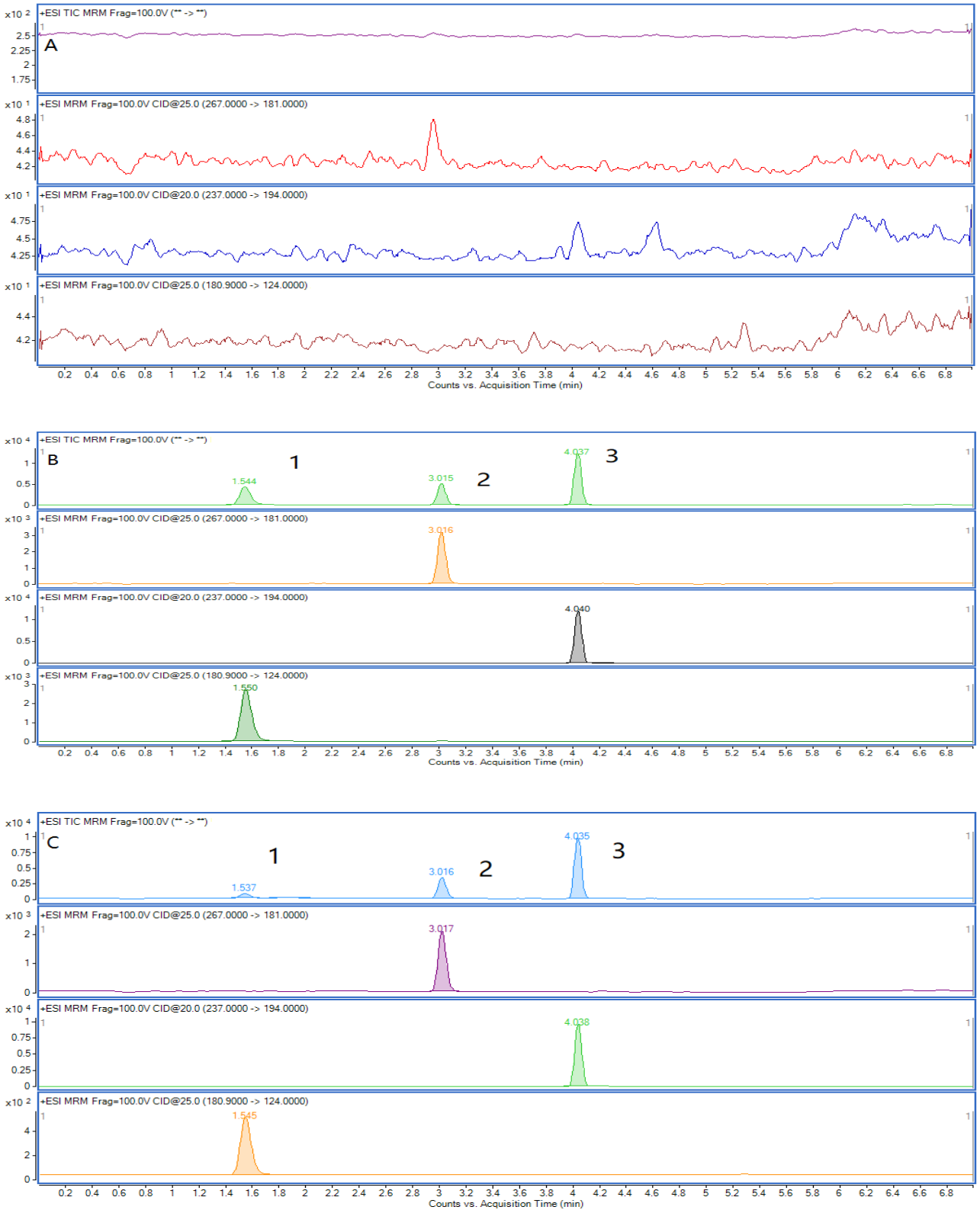

Fig. 2: Chromatograms of doxofylline and its metabolite in rat plasma. (A) Blank plasma sample; (B) Standard plasma sample spiked with doxofylline, theophylline and carbamazepine; (C) Plasma sample; 1: Carbamazepine; 2: Doxofylline; 3: Theophylline.

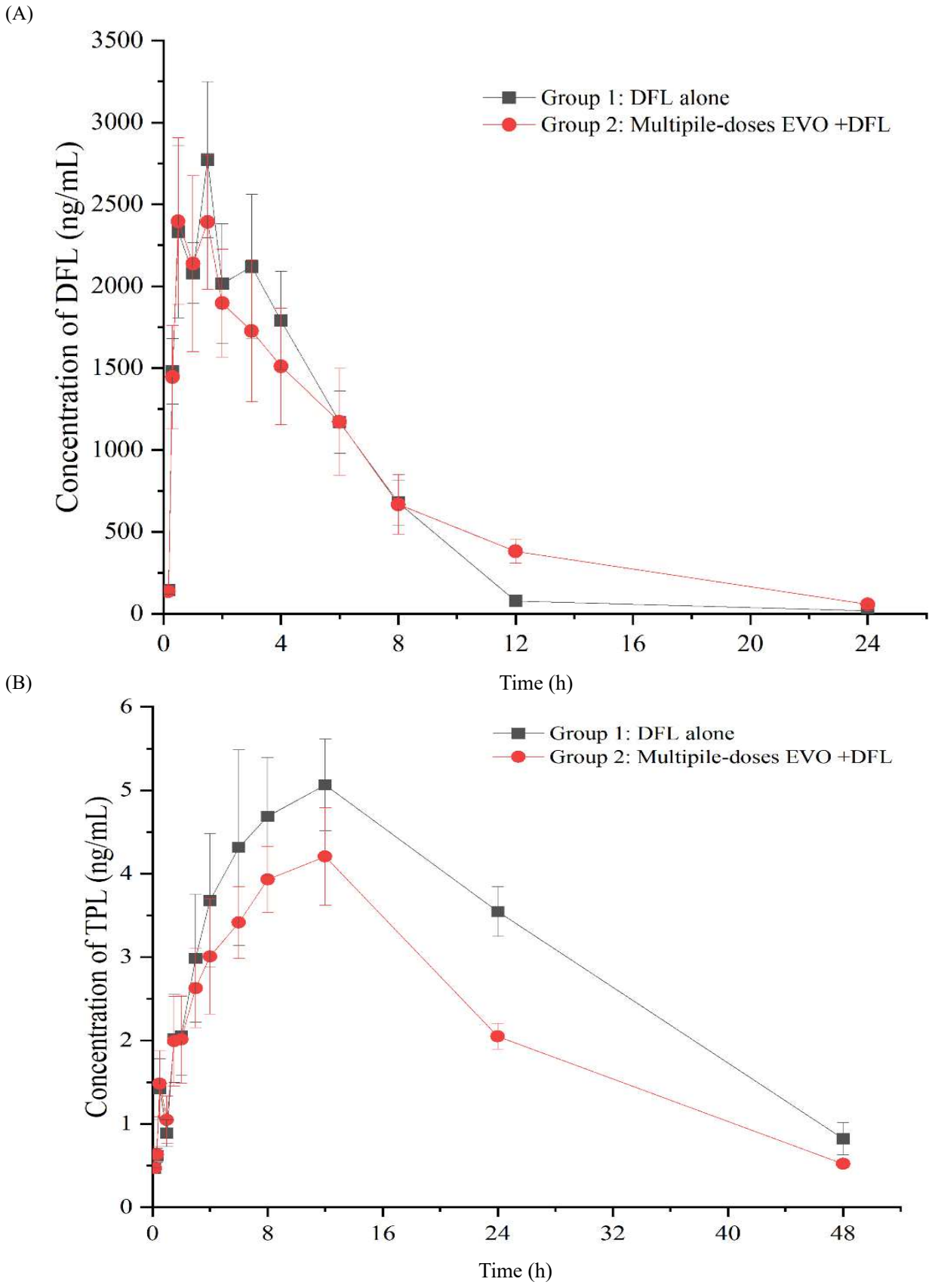

Fig. 3: Mean plasma concentration-time curves of (a) DFL and (B) TPL in two groups (n=6).

Table 1: Intra-day and inter-day precision and accuracy of DFL and TPL in rat plasma (n=5).

Analytes	Concentration ($ng \cdot mL^{-1}$)	Intra-day		Intre-day	
		Mean ±SD (%)	RSD (%)	Mean±SD (%)	RSD (%)
DFL	20	19.59±0.74	3.75	19.92±0.0.69	3.46
	500	499.26±17.74	3.55	505.89±30.42	6.01
	2000	2018.31±85.23	4.22	2008.28±56.20	2.80
TPL	2.5	2.44±0.09	3.88	2.40±0.10	4.30
	7.5	7.36±0.22	2.92	7.53±0.14	1.89

Table 2: Extraction recovery and matrix effects of DFL and TPL in rat plasma (n=5).

Analytes	Concentration ($ng \cdot mL^{-1}$)	Extraction recovery		Matrix effects	
		Mean±SD (%)	RSD (%)	Mean±SD (%)	RSD (%)
DFL	20	96.53±7.76	8.04	101.08±7.37	7.30
	500	95.63±7.88	8.24	97.00±5.45	5.62
	2000	91.19±4.25	4.66	98.84±5.08	5.14
TPL	2.5	103.38±8.87	8.58	100.31±5.05	5.04
	7.5	96.09±4.75	4.95	99.30±4.32	4.35
	15	94.08±8.03	8.54	102.11±6.85	6.71

Table 3: Pharmacokinetic parameters of DFL and TPL in rats after oral administration alone and combined with EVO.2.

Pharmacokinetic parameters	DFL		TPL	
	Group 1	Group 2	Group 1	Group 2
$AUC_{(0-t)}$ (ng·h/mL)	14932.446±1265.748	16522.796±2473.729	149.083±13.902	106.244±7.573**
$AUC_{(0-\infty)}$ (ng·h/mL)	15007.042±1273.384	16889.522±2487.814	168.937±18.164	116.08±5.613**
$t_{1/2z}$ (h)	2.959±0.145	4.376±0.46**	16.155±3.219	12.859±1.969
T_{max} (h)	1.25±0.612	0.917±0.492	10.333±2.658	11.333±1.633
CLz/F (L/h/kg)	0.0053±0.00052	0.0046±0.00082	0.478±0.053	0.691±0.031**
Vz/F (L/kg)	0.023±0.002	0.031±0.007*	11.096±2.302	12.867±2.397
C_{max} ($mg \bullet L^{-1}$)	2964.422±393.124	2644.362±463.393	5.268±0.782	4.35±0.385*
$MRT_{(0-t)}$ (h)	4.28±0.163	5.758±0.322**	17.924±1.013	16.552±0.498*
$MRT_{(0-\infty)}$ (h)	4.399±0.154	6.299±0.346**	23.54±3.467	20.831±1.83*
$VRT_{(0-t)}$ (h^2)	10.867±0.795	21.925±1.617**	117.278±12.163	118.632±8.0495
$VRT_{(0-\infty)}$ (h^2)	13.76±1.285	35.431±5.594**	432.057±183.24	337.797±92.307

Note: *P<0.05, **P<0.01 = significant in comparison to control group.

DISCUSSION

Asthma, a quintessential chronic condition, is marked by bronchial hyper-responsiveness stemming from pulmonary inflammation. Proper management can significantly enhance the quality of life for asthmatic patients. Typically, they are prescribed a combination of Western medicines and traditional herbal remedies to alleviate airway inflammation. However, polypharmacy may alter drug profiles concerning pharmacodynamics and pharmacokinetics due to potential drug interactions, which could compromise efficacy, increase adverse events, induce toxicity, and even lead to hospitalization. Identifying these interactions is crucial to minimize the risk of adverse outcomes.

The focus on natural molecules for their therapeutic potential continues to rise. EVO, a naturally occurring alkaloid with a quinazolinocarboline structure, is prevalent in Evodia rutaecarpa and Euonymus europaeus (Haiss *et al.,* 2025; Zhao *et al*., 2020). Its earliest documentation was traced back to Shennong's Classic of Materia Medica, and it is commonly employed in TCM to alleviate headaches and dizziness (Cao *et al.*, 2023). CYP1A2 and CYP3A4 are the primary CYP isoforms engaged in EVO metabolite processing in hepatic microsomes (Panda *et al.,* 2023). An animal experiment showed that EVO had an inhibitory effect on CYP1A2, CYP2C9, and CYP2D6, with no substantial effect on CYP3A4 and CYP2C19 (Zhang *et al.,* 2016). However, another study indicated that the formation of evodiamine glutathione (GSH) conjugates mainly depended on the catalysis of heterologously expressed recombinant CYP3A4, while a small portion of it relied on CYP1A2 and CYP2D6 (Wen *et al.,* 2014). This suggests that the metabolic process of EVO in liver microsomes is complex and may diversely affect the metabolism of other drugs through CYP. Prior research has shown that EVO suppresses the metabolism of dapoxetine. The reason why the metabolism of dapoxetine may be affected is that dapoxetine serves as a catalytic substrate for CYP3A4 in both the intestinal and hepatic systems (Li *et al.,* 2016). Presumably, EVO can bind to CYP3A4, occupying the active center of the enzyme and thus hindering the normal metabolism of dapoxetine. Besides, EVO diminished the

distribution of pravastatin within the body by upregulating the expression of organic anion transporting polypeptides (OATPs) (Liang *et al.*, 2022), with no transportation through P-glycoprotein (p-gp), which means EVO merely has a light or medium grade effect on p-gp (Wang *et al.*, 2021). This suggests that drug transporters are another target site, where EVO affects the metabolism of other drugs.

DFL is a derivative of methylxanthine, metabolized in the liver to TPL and theophylline-7-acetic acid-2-hydroxyethyl ester, and further converted into uric acid derivatives, which are ultimately eliminated through urine. Studies have confirmed that DFL and its metabolite TPL are primarily metabolized via the CYP1A2 pathway (Li *et al*., 2013). Consequently, any substance affecting CYP1A2 may affect the metabolism of DFL and TPL. Rat experiments have shown that OATP expression levels do not affect the absorption and distribution of TPL (Takeda et al., 2021) and that TPL is not a substrate of p-gp but is passively permeable (Mariappan *et al.*, 2014). In summary, there is a possibility of a PK interaction between EVO and DFL through CYP. Therefore, this experiment aims to investigate the impact of EVO on DFL and the PK of its metabolite TPL *in-vivo*.

As detailed in Table 3, EVO significantly increased the $t_{1/2z}$, Vz/F, $MRT_{(0-t)}$, $MRT_{(0-\infty)}$, $VRT_{(0-t)}$, and $VRT_{(0-\infty)}$ of DFL in the experimental group. Concurrently, the CLz/F of the metabolite TPL was significantly higher in the presence of EVO compared to the control group, while the $AUC_{(0-t)}$, $AUC_{(0-\infty)}$, C_{max}, $MRT_{(0-t)}$, and $MRT_{(0-\infty)}$ values were reduced. These results indicated that DFL was possibly metabolized via the CYP1A2 pathway in the liver, and EVO may retard the metabolism of DFL by inhibiting CYP1A2. The formation and metabolism of TPL, the metabolite of DFL, mainly depend on CYP1A2 and CYP3A4 in the cytochrome P450 enzyme system, while, according to previous studies (Matera et al., 2017), CYP3A4 also plays a crucial role in metabolizing EVO within liver microsomes (Peng *et al*., 2023).

These varied results align with studies showing that EVO is primarily catalyzed by recombinant CYP1A2. Moreover, EVO inhibits DFL metabolism and has a more pronounced effect on its metabolite TPL. EVO significantly inhibits TPL formation in this metabolic system. This inhibitory effect may arise from the specific binding of EVO to CYP3A4, which competes with normal catalytic function and ultimately reduces TPL levels. It may trigger a series of cascading reactions in the *in-vivo* metabolic process of DFL, thereby having a considerable impact on its pharmacodynamic and PK properties. More specifically, this inhibitory effect will change the performance of DFL in aspects such as the duration, intensity, and metabolic clearance rate *in-vivo*. The conclusions regarding the involvement of drug-metabolizing enzymes, particularly CYP1A2 and CYP3A4, remain preliminary. This interpretation is based primarily on *in-vivo* PK observations, while also being consistent with literature on relevant metabolic pathways. However, definitive mechanistic evidence from controlled *in-vitro* studies is lacking. Therefore, the attribution of metabolic clearance to these specific cytochrome P450 isoforms is inferential. Future studies should include systematic *in-vitro* investigations to definitively characterize the enzymes' contributions and confirm their proposed roles.

Meanwhile, as shown in Fig. 3, at the 48 h blood time point, the plasma concentration of the parent compound DFL declined below the LLOQ, whereas its metabolite TPL remained quantifiable. This differential PK behavior arises primarily from distinct disposition characteristics between DFL and TPL. DFL exhibits a shorter $t_{1/2}$, a reduced MRT, and a higher systemic clearance, leading to rapid elimination from systemic circulation. In contrast, TPL demonstrates a longer elimination $t_{1/2}$ and prolonged MRT. Moreover, TPL is continuously supplied via slow, sustained conversion from tissue-resident DFL pools and other metabolic pathways, thereby sustaining measurable plasma concentrations over an extended period. Consequently, further clinical research is imperative to assess the potential herb-drug interactions when EVO and DFL are administered concurrently, as suggested by the findings of this study. As this study was conducted using a rodent model, the translational relevance of its findings to human clinical practice requires further rigorous validation.

CONCLUSION

In the present study, we refined a rapid and sensitive LC-MS/MS method for the simultaneous quantification of DFL and TPL in plasma samples. This analytical approach was successfully applied to PK interaction studies of DFL. The results revealed that co-administration of DFL with multiple doses of EVO partially inhibited DFL metabolism, without significantly increasing its systemic bioavailability; meanwhile, EVO markedly accelerated the metabolic clearance of TLP. Together, these findings substantiate a probable PK interaction between EVO and DFL, likely mediated through comparative inhibition and enzyme induction involving shared CYP450-dependent metabolic pathways. Hence, dose adjustments should be carefully considered when EVO and DFL are administered concomitantly. It should be noted, however, that this study is preclinical in nature and does not address the underlying inflammatory mechanisms. Further rigorous clinical trials are warranted to validate the observed interactions between EVO and DFL and to elucidate their clinical relevance for informed treatment decisions.

Acknowledgements
None.

Authors' contributions

Yuxian Lin: Designed the study and wrote the original manuscript as well as the review and editing; Yongle Yang and Wang Luo: Collected the data and handled the statistical analysis; Yangfang Chen and Feng Chen: Designed the methodology and wrote the review and editing; Zhenyang Zang and Qiulian Tang: Collected animal blood samples.

Funding

This research is supported by the Foundation of the Zhejiang Provincial Medical and Health Science and Technology Planning Project of China (2025KY1513), the Shanghai Rehabilitation Medical Association's Outstanding Young Talent Development Program in Health Management (2024JGYQ08) and the Science and Technology Plan Project of Wenzhou (Grant No. Y2023188).

Data availability statement

The datasets generated during and/or analyzed during the current study are available from the corresponding author on reasonable request.

Ethical approval

The animal experiment protocols were approved by the Institutional Animal Ethics Committees of Yantai University (Approval No. 20250516). This study was performed in adherence with the ARRIVE guidelines. See supplementary file for the ARRIVE checklist.

Conflict of interest

The authors declare no conflict of interest.

Supplementary data

https://www.pjps.pk/uploads/2026/06/SUP1781607498.pdf

REFERENCES

Al-Shami A, Mohamed MA, Ma H, Nejad SK, Soleimani A, Amirghasemi F, Banks M, Garcia D, Tasso A, Yaseen AA and Mousavi MPS (2025). quantification theophylline A point-of-care device for in human milk using laser-induced graphene electrodes. *ACS. Appl. Nano. Mater.*, **8**(22): 11447-11457.

Campbell JL Jr, Travis KZ, Clewell HJ 3rd, Stevens AJ, Hinderliter PM andersen ME, Botham PA, Cook AR, Minnema DJ and Wolf DC (2021). Integration of paraquat pharmacokinetic data across species using PBPK modelling. *Toxicol. Appl. Pharmacol.*, **417**: 115462.

Cao Q, Liu J, Dong P and Han H (2023). Different ratios of schisandra combination for treating Alzheimer's disease chinensis and evodia rutaecarpa. *Exp. Biol. Med (Maywood)*, **248**(20): 1877-1886.

Castillo-Ribelles L, Arranz-Amo JA, Hernandez-Vara J, Ferrer-Costa R, Martinez-Vicente M and Carnicer-Caceres C (2025). Systematic assessment of matrix effect, recovery and process efficiency using three complementary approaches: Implications for LC-MS/MS bioanalysis applied to glucosylceramides in human cerebrospinal fluid. *ACS Omega.*, **10**(44): 52449-52458.

Fang LN, Mao MQ, Zhao XH, Yang L, Jia H, Xia SY (2019). Development and validation of a UPLC-MS/MS method for quantification of doxofylline and its metabolites in human plasma. *J. Pharm. Biomed. Anal.*, **174**: 220-225.

Fierro V, Piscitelli AL, Battaglia E and Fiocchi A (2022). Doxofylline for pediatric asthma steps 1-4. pediatric asthma: New role for an dld drug. *Front. Pediatr.*, **10**:772704.

Haiss P, Liu R, Xian F, Varela DG, Schmidt M, Dirsch VM and Blazevic T (2025). Evodiamine induces centrosome amplification with subsequent G2/M cell cycle arrest in primary vascular smooth muscle cells. *Biochem. Pharmacol.*, **242**(Pt 2): 117320.

Harstad E andaya R, Couch J, Ding X, Liang X, Liederer BM, Messick K, Nguyen T, Schweiger M, Tarrant J, Zhong S and Dean B (2016). Balancing blood sample volume with 3Rs: Implementation and best practices for small molecule toxicokinetic assessments in rats. *ILAR J.*, **57**(2):157-165.

Li RF, Fu JM, Lv XZ, Zhang DT, Pan YY, Rao DP and Yu KY (2016). Effects of evodiamine on the pharmacokinetics of dapoxetine and its metabolite desmethyl dapoxetine in rats. *Pharmacology*, **97**(1-2): 43-7.

Li XP, Zhang CL, Gao P, Gao J and Liu D (2013). Effects of andrographolide on the pharmacokinetics of aminophylline and doxofylline in rats. *Drug Res (Stuttg)*, **63**(5): 258-62.

Liang R, Ge W, Li B, Cui W, Ma X, Pan Y and Li G (2022). Evodiamine decreased the systemic exposure of pravastatin in non-alcoholic steatohepatitis rats due to the up-regulation of hepatic OATPs. *Pharm. Biol.*, **60**(1): 359-373.

Liu CY, Wu JH, Chen ZY, Zhang Y, Huang CL, Lin AM, Xu XT and Gao XH (2021). Effect of doxofylline on reducing the inflammatory response in mechanically ventilated rats with chronic obstructive pulmonary disease. *Int. J. Chron. Obstruct. Pulmon. Dis.*, **16**: 2375-2383.

Ma YJ, Jiang DQ, Meng JX, Li MX, Zhao HH, Wang Y and Wang LQ (2016). Theophylline: A review of population pharmacokinetic analyses. *J. Clin. Pharm. Ther.*, **41**(6): 594-601.

Mariappan TT, Kurawattimath V, Gautam SS, Kulkarni CP, Kallem R, Taskar KS, Marathe PH and Mandlekar S (2014). Estimation of the unbound brain concentration of P-glycoprotein substrates or nonsubstrates by a serial cerebrospinal fluid sampling technique in rats. *Mol. Pharm.*, **11**(2): 477-85.

Matera MG, Page C and Cazzola M (2017). Doxofylline is

not just another theophylline. *Int. J. Chron. Obstruct. Pulmon. Dis.*, **12**: 3487-3493.

Moreira LN, Feltrin C, Gonçalves JE, de Castro WV, Simoes CMO, de Padua RM, Cortes SF and Braga FC (2020). Determination of l-(+)-bornesitol, the hypotensive constituent of *Hancornia speciosa*, in rat plasma by LC-MS/MS and its application on a pharmacokinetic study. *Biomed. Pharmacother.,* **132**: 110900.

Panda M, Tripathi SK, Zengin G and Biswal BK (2023). Evodiamine as an anticancer agent: A comprehensive review on its therapeutic application, pharmacokinetic, toxicity and metabolism in various cancers. *Cell Biol Toxicol*, **39**(1): 1-31.

Papadopoulos NG, Miligkos M and Xepapadaki P (2022). A current perspective of allergic asthma: From mechanisms to management. *Handb. Exp. Pharmacol.*, **268**: 69-93.

Peng T, Rao J, Zhang T, Wang Y, Li N, Gao Q, Feng X, Song Z, Wang K and Qiu F (2023). Elucidation of the relationship injury and CYP3A4-mediated metabolic liver evodiamine-induced between activation by UPLC-MS/MS analysis. *Anal. Bioanal. Chem.*, **415**(23): 5619-5635.

Rao RN, Prasad KG, Naidu ChG, Saida S and Agwane SB (2013). Development of a validated on rat dried blood spots doxofylline LC-MS/MS method for determination of urine: Application to pharmacokinetics. *J. Pharm. Biomed. Anal.*, **78-79**: 211-6.

Sun Q, Xie L, Song J and Li X (2020). Evodiamine: A review of its pharmacology, toxicity, pharmacokinetics and preparation researches. *J. Ethnopharmacol.*, **262**: 113164.

Takeda F, Oda M, Terasaki M, Kubota A, Asada K, Ichimura Y, Kojima H and Saitoh H (2021). Downregulated expression of organic anion transporting polypeptide (Oatp) 2b1 in the small intestine of rats with acute kidney injury. *Drug Metab. Pharmacokinet.*, **40**: 100411.

Wang Q, Cui Y, Wu X and Wang J (2021). Evodiamine protects against airway remodelling and inflammation in asthmatic rats by modulating the HMGB1/NF-κB/TLR-4 signalling pathway. *Pharm. Biol.*, **59**(1): 192-199.

Wang T, Qi D, Hu X, Li N, Zhang X, Liu H, Zhong C and Zhang J (2021). A novel evodiamine amino derivative as a PI3K/AKT signaling pathway modulator that induces apoptosis in small cell lung cancer cells. *Eur. J. Pharmacol.*, **906**:174215.

Wen B, Roongta V, Liu L and Moore DJ (2014). Metabolic activation of the indoloquinazoline alkaloids evodiamine and rutaecarpine by human liver microsomes: Dehydrogenation and inactivation of cytochrome P450 3A4. *Drug Metab. Dispos.*, **42**(6): 1044-54.

Wu TD, Brigham EP and McCormack MC (2019). Asthma in the primary care setting. *Med. Clin. North. Am.*, **103**(3): 435-452.

Yang KH, Lee JH and Lee MG (2008). Effects of CYP inducers and inhibitors on the pharmacokinetics of intravenous theophylline in rats: Involvement of CYP1A1/2 in the formation of 1,3-DMU. *J. Pharm. Pharmacol.*, **60**(1): 45-53.

Yang Y, Wu P, Guo J, Pan Z, Lin S, Zeng W, Wang C, Dong Z and Wang S (2024). Circadian disposition and theophylline time-dependent effects of experimental colitis on toxicity. *Br. J. Pharmacol.*, **181**(19): 3743-3759.

Yuxian LIN, Peipei PAN, Jianhua XIONG, Lianguo CHEN, Qiong WANG, Shujun WANG, Lirong SUN and Guoxin HU (2015). Alcohol affects the pharmacokinetics of doxofylline and its metabolite theophylline in rats. *Lat. Am. J. Pharm.*, **34**(6): 1065-1069.

Zha Y, Yang Y, Zhou Y, Ye B, Li H and Liang J (2023). Dietary Evodiamine inhibits atherosclerosis-associated changes in vascular smooth muscle cells. *Int. J. Mol. Sci.*, **24**(7): 6653.

Zhang YT, Zhang DF, Ge NY, Zhu GH, Hao C, Zhang Y and Chen RJ (2016). Effect of evodiamine on CYP enzymes in rats by a cocktail method. *Pharmacology*, **97**(5-6): 218-23.

Zhao J, Zhang Q, Zou G, Gao G and Yue Q (2020). Corrigendum to "Arenobufagin, isolated from toad venom, inhibited epithelial-to-mesenchymal transition and suppressed migration and invasion of lung cancer cells via targeting IKKβ/NFκB signal cascade". *J. Ethnopharmacol.*, **250**(25): 112492

Zhao X, Ma H, Pan Q, Wang H, Qian X, Song P, Zou L, Mao M, Xia S, Ge G and Yang L (2020). Theophylline acetaldehyde as the initial product in doxophylline metabolism in human liver. *Drug Metab. Dispos.*, **48**(5): 345-352.